

Dissociation of I Domain and Global Conformational Changes in LFA-1: Refinement of Small Molecule-I Domain Structure–Activity Relationships[†]

Richard S. Larson,^{*,‡} Terry Davis,[§] Cristian Bologa,^{||} Gloria Semenuk,[‡] Sreejith Vijayan,[‡] Yu Li,[‡] Tudor Oprea,^{||} Alexandre Chigayev,[‡] Tione Buranda,[‡] Carston R. Wagner,[§] and Larry A. Sklar[‡]

Department of Pathology, University of New Mexico, and Cancer Research and Treatment Center, Albuquerque, New Mexico 87131-5301, Department of Biochemistry, Division of Biocomputing, University of New Mexico, Albuquerque, New Mexico 87131-5301, and Department of Medicinal Chemistry, University of Minnesota, Minneapolis, Minnesota 55455

Received August 20, 2004; Revised Manuscript Received January 24, 2005

ABSTRACT: LFA-1 ($\alpha\beta 2$) is constitutively expressed on leukocytes, but its activity is rapidly regulated. This rapid activation has been proposed to be associated with conformation changes in the inserted (“I”) domain within the headpiece of LFA-1 as well as conversion of the molecules from bent to extended forms. To study these molecular changes as they relate to affinity regulation of LFA-1, we developed and synthesized a fluorescent derivative of BIRT-377 [Kelly et al. (2001) *J. Immunol.*] to examine changes in LFA-1 affinity in a flow cytometer with live cells. BIRT-377 binds to the ligand-binding or “I” domain of LFA-1. Structure–activity relationships studies indicated that an aminoalkyl group could be added to the central hydantoin group without significantly affecting binding. Using this modified derivative [1-(*N*-fluoresceinylthioureidobutyl)-[5*R*]-[4-bromobenzyl]-3-(3,5-dichlorophenyl)-5-methyl-imidazolidine-2,4-dione (FBABIRT)], we analyzed the affinity of FBABIRT binding to LFA-1 on live cells. The binding affinity increases, and the dissociation rate decreases with divalent cation (Mn^{2+}) stimulation. We then used FBABIRT with fluorescent resonance energy transfer (FRET) to show that LFA-1 changes its height relative to the cell surface when cells were treated with dithiothreitol (DTT) but not Mn^{2+} . Competition assays among FBABIRT and BIRT derivatives defined structure–affinity relationships that refine the current model of BIRT-377 binding to the I domain. Our data supports the model in which BIRT-377 binds to the I domain and stabilizes the bent structure of LFA-1, while divalent cation activation results in a small conformational change in the I domain without significant extension of LFA-1. DTT, in contrast, induces a conversion to the extended form of LFA-1 in the presence of BIRT-377 on live cells. The structure–activity studies suggest that BIRT-377 is a fully optimized inhibitor.

Integrins are a family of cell-surface receptors composed of covalently associated $\alpha\beta$ heterodimers that contribute to embryogenesis, organ formation, immune function, and angiogenesis (1, 2). The leukocyte integrin, LFA-1 ($\alpha\beta 2$), is a member of the leukocyte integrin subfamily that shares a common $\beta 2$ subunit among four members, LFA-1 ($\alpha\beta 2$), Mac-1 ($\alpha\text{m}\beta 2$), p150 ($\alpha\text{x}\beta 2$), and αd ($\alpha\text{d}\beta 2$). LFA-1 is exclusively expressed on leukocytes and is important in a variety of cell–cell adhesion events including leukocyte binding to endothelium during extravasation and in the formation of the immunologic synapse between antigen presenting and T cells (3–5). A genetic defect in the $\beta 2$

subunit that prevents or markedly reduces expression of leukocyte integrins, leukocyte adhesion deficiency (LAD), leads to a potentially life-threatening immunodeficiency (6). As a result, LFA-1 has gained considerable attention as a molecular target for attenuation of overactive immune responses and inflammatory diseases. Recent publications have reported positive results in animal models of transplantation (7–9) and in human trials of psoriasis (10, 11).

Each of the leukocyte integrins has an inserted (“I”) domain in the α subunit and an I-like domain in the β subunit (12). Each domain forms a Rossmann fold with a metal-ion-dependent adhesion site (MIDAS). In this class of integrins, the affinity of the I domain is regulated by a 10 Å downward displacement of the C-terminal ($\alpha 7$) helix, which is conformationally linked to alterations of MIDAS loops and divalent cation coordination (13–16). The downward displacement promotes a shift from a “closed” to an “open” conformation of the I domain that more readily binds its ligand, ICAM-1. The $\beta 2$ I-like domain does not directly bind ligand despite containing a MIDAS motif. Instead, it functions indirectly by regulating the activity of the I domain (16). Recent studies have also suggested that activation causes the $\alpha\beta$ heterodimer of the LFA-1 to transition from

[†] This work has been supported by ACS RPG-00-096-01-LBC (to R.S.L.), NIH RR14175 (to L.A.S.), NIH EB02022 (to L.A.S.), NIH HL56384 (to L.A.S.), and Ziagen University of Minnesota Faculty Development Grant (to C.R.W.).

^{*} To whom correspondence should be addressed: University of New Mexico, Department Pathology, 2325 Camino de Salud, CRF 223, Albuquerque, NM 87112. Telephone: (505) 272-9762. Fax: (505) 272-9762. E-mail: rlarson@salud.unm.edu.

[‡] Department of Pathology, University of New Mexico, and Cancer Research and Treatment Center.

[§] University of Minnesota.

^{||} Department of Biochemistry, Division of Biocomputing, University of New Mexico.

a bent to an extended form in a "switchblade-like" process (16, 17). In this transition from a bent to an extended form, the I domain of the α subunit of LFA-1 shifts from a closed to an open conformation. Thus, with activation, the receptor extends upward exposing an I domain in the open conformation that can bind ligand with higher affinity.

Two classes of allosteric LFA-1 inhibitors have been described to date. Direct competitive inhibitors have not been described. The first LFA-1 small molecule inhibitor to be described was BIRT-377 and represents the first class of antagonists that bind the I domain of the α subunit and stabilizes a low-affinity state (18–22). This class also includes a number of statin-derived molecules. The second class of compounds has only recently been developed and binds the I-like domain of the β 2 subunit and prevents its conformational signals to the I domain (23–26). Thus, the second class inhibits all four members of the leukocyte integrin family. Integrated studies using immunochemical, chemical, and molecular-modeling approaches have indicated that BIRT-377 binds at and forms close contacts with the C-terminal α 7 helix of the I domain within a 30 Å cubic area with the center defined in the proximity of proline 281 (18, 27). This site is located on the protein surface opposite to the ICAM-binding site, which is located near the MIDAS domain. Structure–activity studies to date suggest that BIRT-377 binds to LFA-1 solely through nonionic interactions (18). Two hydrophobic pockets in the I domain interact with the aromatic rings of BIRT-377 in an edge to face aromatic/aromatic orientation. This binding presumably prevents displacement of the α 7 helix and overall conformational changes of the whole protein stabilizing it in the bent, low-affinity state.

Because of the key role of LFA-1 and ICAM-1 interaction in immune and inflammatory diseases, there is great interest in understanding the structural basis of LFA-1 activation and inhibitors of that activation. We have previously used fluorochrome-labeled small molecules to probe the structure–affinity relationships of the α 4 β 1 integrin (28, 29). In this study, we wished to determine whether a fluorescein-labeled BIRT-377 derivative could be used to refine our understanding of the structural features and conformational changes of LFA-1 in the presence and absence of pharmaceutical inhibitors on live cells. Using a series of structural and pharmacologic manipulations, we show that the conformational change in the I domain can occur independently of the conversion from a bent to an extended form. In addition, our structure–affinity studies using derivatives of BIRT refine previously proposed models of BIRT binding.

EXPERIMENTAL PROCEDURES

Cell Lines. U937 Δ ST was a kind gift of Dr. E. Prossnitz (UNM, Albuquerque, NM). HL60 cells were purchased from American Tissue Culture Corporation (Manassas, VA). Cells were cultured at 37 °C in a humidified atmosphere of 5% CO₂ and 95% air. Cells were grown in RPMI 1640 supplemented with 2 mM L-glutamine, 100 units/mL penicillin, 100 μ g/mL streptomycin, 10 mM HEPES at pH 7.4, and 10% heat-inactivated fetal bovine serum.

Monoclonal Antibodies. R7.1 was a kind gift of R. Rothlein (Boehringer Ingelheim, Torrence, CT). TS1/22 was produced from hybridomas as previously described (43). Fab

fragments of TS1/22 were produced using a commercial kit based on ficin digestion (ImmunoPure IgG1 Fab and F(ab)₂ Preparation Kit, Pierce Biotechnology, Rockford, IL) per recommendations of the manufacturer. Purity of the Fab fragment was verified by SDS–PAGE analysis. TS1/22 Fab fragments were labeled with fluorescein isothiocyanate (FITC) using Quick tag FITC Conjugation kit (Roche Diagnostics Corp, Indianapolis, IN).

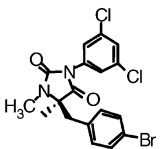
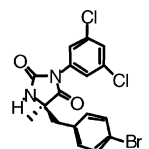
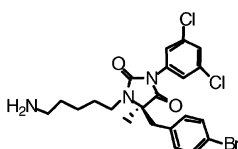
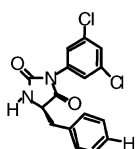
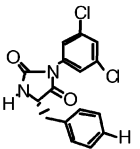
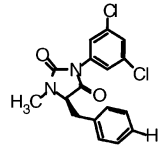
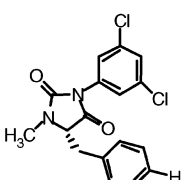
Synthesis of BIRT-377 and BIRT Derivatives. BIRT-377 was a gift of T. Kelly (Boehringer Ingelheim) (18) or was synthesized *de novo* (Wagner et al., manuscript in preparation). Compounds **I–VI** were prepared and shown to be greater than 99% pure by HPLC and optically pure by polarimetry (Table 1; Wagner et al., manuscript in preparation). The product, FBABIRT was isolated by chromatography on a 10 g bed RP-18 gravity column.

1-(4-Aminobutyl)-5-(4-bromobenzyl)-3-(3,5-dichlorophenyl)-5-methyl-imidazolidine-2,4-dione (Compound **I).** Compound **I** was converted to 2-[4-[5-(4-bromo-benzyl)-3-(3,5-dichloro-phenyl)-5-methyl-2,4-dioxo-imidazolidin-1-yl]-butyl]-phthalimide by the method of ref 18 followed by aminolysis to compound **II** by the method of ref 18 (Scheme 1).

1-(N-Fluoresceinylthioureidobutyl)-[5R]-(4-bromobenzyl)-3-(3,5-dichlorophenyl)-5-methyl-imidazolidine-2,4-dione, Triethylammonium salt (FBABIRT). To 75 mg (0.150 mmol) of aminobutylhydantoin (**II**) in 1 mL of dry tetrahydrofuran (THF) was added 1.05 eq of 58.5 mg of fluorescein isothiocyanate (isomer **I**, Aldrich Chemical Co., catalog F250-2, Milwaukee, WI) in 1 mL of abs alcohol (Scheme 1). To this was added, dropwise, a 50-fold excess of triethylamine (TEA, 1 mL, 7.17 mmol). The reaction was stirred at room temperature for 4 h, and then the solvent was removed by evaporation [TLC (RP-18, 20% H₂O/MeOH, 1 drop TEA/0.10 mL, vis detxn) FITC reagent, *R_f* 0.80; product, *R_f* 0.20]. Applied to 10 g bed RP-18 Sep-Pak (Supelco Co., Bellefonte, PA), fluoresceinthiourea TEA salt was eluted by 20% H₂O/MeOH and 0.2 mL TEA/100 mL, and then the product was eluted by 10% H₂O/MeOH to give 120 mg (80% yield) of FBABIRT as a chromatographically pure, red-orange glass. The product could be crystallized from MeOH to give orange needles, mp 260 °C (dec). ¹H NMR (CD₃OD): 7.94, s 1H; 7.64, 1s, dd (*J* = 8.1, 2.3 Hz); 7.41, 2H, dd, (*J* = 8.1, 2.3 Hz); 7.35, 1H, t (*J* = 1.8 Hz); 7.15, 1H, d (*J* = 8.2 Hz); 7.10, 2H, dd (*J* = 9.0, 3.8 Hz); 7.00, 2H, dd (*J* = 8.4, 1.8 Hz); 6.84, 2H, d, (*J* = 1.8 Hz); 6.59–6.56, 4H, m; 3.75, 2H, M; 3.70, 1H, m; 3.52, 1H, m; 3.23, 1H, d (*J* = 17 Hz); 3.00, 1H, d, (*J* = 17 Hz) (presence under TEA peaks disclosed by GCOSY and HMQC); 3.00, 6H, q (*J* = 7.3 Hz); 1.86, 1H, m; 1.77, 3H, m; 1.67, 3H, s; 1.12, 15H, t (*J* = 7.3 Hz). MS: (positive ion mode) (C₄₂H₃₄N₄BrCl₂O₇S, calculated 887.070, observed 887.068, error 3.96 ppm; (M + Na): C₄₂H₃₃N₄BrCl₂O₇SNa, calculated 909.052, observed 909.051, error 1.38 ppm. Observed isotopic peaks are consistent with the composition.

Equilibrium Binding of FBABIRT. For equilibrium binding studies of FBABIRT, HL60 cells were treated with a range of concentrations (1–500 nM) of the fluorescent peptide in the presence or absence of 1 mM MnCl₂. Incubations were performed for short times at room temperature and on ice with qualitatively similar results. Because the equilibration time of high-affinity molecules is typically a function of their dissociation rate, we have found it experimentally convenient

Table 1: Activity of BIRT-377 and Its Derivatives

compound	structure	EC ₅₀ (nM ^a)	IC ₅₀ (μM ^b)
BI RT-37 7		13.7 ± 4	0.3
I		17.5 ± 5	>10
II		35.6 ± 18	0.3
III		402 ± 66	4.2
IV		1708 ± 409	>10
V		245 ± 42	3.2
VI		529 ± 50	4.5

^a EC₅₀, concentration necessary to inhibit 50% binding to LFA-1.^b IC₅₀, concentration necessary to inhibit cellular homotypic aggregation by 50%.

to perform either 1 h or overnight incubations. Nonspecific binding was determined using a 500-fold excess of unlabeled Butylamino-NorBIRT (II, Table 1). Analysis was performed on a FACScan (Becton–Dickinson), and 10 000 events were acquired. Because instrument sensitivity was varied between experiments, the mean channel fluorescence values are not comparable.

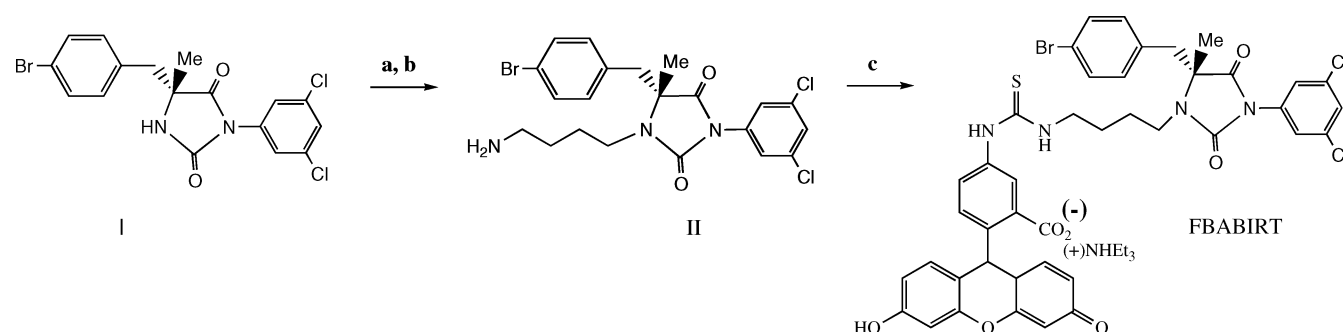
Kinetic Analysis of FBABIRT Binding and Dissociation by FACS Analysis. HL60 cells (1×10^6 mL⁻¹) were preincubated with 100–200 nM FBABIRT for 30 min on ice and 500 rpm stirring. Flow cytometric analysis was performed continuously for up to 1000 s. The samples were

analyzed for 30–240 s to establish a baseline, and then the stimulus (Mn²⁺) was added and FACS acquisition was immediately re-established (losing 5–10 s of the total time course). For dissociation kinetic measurements, cell samples preincubated with FBABIRT were treated with 500-fold excess (50 μM) unlabeled Butylamino-Nor BIRT, and the dissociation of the fluorescent peptide was followed. The resulting data were converted to mean channel fluorescence over time using Tru-Rate software developed by Seamer and Sklar or using FACSQuery software developed by B. Edwards (28). Curve fits and statistics were performed using GraphPad Prism 6.0 (San Diego, CA).

Calibration of Surface Markers. Expression of LFA-1 was measured by fluorescent mAb's and quantified by comparison with standard curves generated with Quantum Simply Cellular microspheres (Flow Cytometry Standards, San Juan, Puerto Rico) stained in parallel with the same mAb. This produces an estimate of the total mAb-binding sites/cells (30).

Calibration of FBABIRT Binding. Quantum 24 Premix Microbeads (Flow Cytometry Standards Corp.) were used to quantify the fluorescence intensity of cells bearing FBABIRT. One or two drops of beads were added to 0.5 mL of isotonic phosphate-buffered saline (pH 7.2), and the mean channel numbers of all calibrated microbeads were collected. The number of molecules of equivalent soluble fluorochromes was plotted versus the mean channel numbers for the four fluorescent microbeads. The graph was used to estimate the total number of molecules of equivalent soluble fluorochromes/cell.

Fluorescence Resonance Energy Transfer (FRET) Studies. FRET is a distance-dependent interaction between the electronic states of two chromophores in which excitation is transferred from an excited donor molecule (e.g., fluorescein) to an acceptor (A) molecule (e.g., rhodamine) without emission of a photon. In these experiments, the final quenching curves generated characterize the distance of the closest approach between the integrin α subunit I domain where FBABIRT binds and the surface lipid membrane. In the FRET assay performed here, the excited state donors in this work are FBABIRT (or FITC-labeled FAB TS1/22) bound to LFA-1 and the acceptor R18 is a rhodamine-containing lipid that is incorporated into the cell membrane. For FRET experiments, HL60 cells were incubated with 100 nM FBABIRT, 100 nM LDV–FITC (α4 or VLA-4 specific peptide), or FITC–Fab TS1/22 in HHB buffer (30 mM HEPES buffer containing 0.1% human serum albumin supplemented with 1.5 mM CaCl₂ and 1 mM MgCl₂) for 1 h at room temperature. Specific fluorescence was determined by subtracting the background fluorescence, which was determined at each concentration of R18 with FBABIRT in the presence of blocking TS1/22 mAb. The donor intensities of different concentrations of R18 (up to 5 μM) were determined after equilibrating for 1 min and were also subtracted from the specific fluorescence intensity on a point by point basis. The specific fluorescent intensity was then normalized by dividing the fluorescence intensity at each fixed concentration of R18 by the fluorescence intensity without R18. The normalized intensity is graphed as a function of the R18 concentration. The details of the analysis of FRET for α4 integrins on cell surfaces has been described elsewhere as well (31).

Scheme 1^a

^a a: LiHMDS, 4-BrBuphtalimide, 80%. b: MeNH₂, 85%. c: fluorescein isothiocyanate, Et₃N, 80%.

Competitive Binding of BIRT Derivatives with FBABIRT. Competitive binding followed approaches described above. For competitive analysis, HL60 cells were mixed with a range of concentrations of nonlabeled BIRT derivatives in the presence of 50 nM FBABIRT. Incubations were performed at room temperature for 1 h or overnight on ice with qualitatively the same results.

Modeling Methods. The docking experiments were performed with the Autodock package version 3.0 (32) using modified coordinates from a previously published X-ray crystal structure of LFA-1 I domain docked with BIRT-377 in InsightII (available from Accelrys Inc., San Diego, CA, <http://www.accelrys.com/insight/>). The computational procedures match those used in previous work (18), and the geometry of BIRT-377 was built in a conformation identical to that previously described on the basis of X-ray crystallography data (18). The geometry was optimized using AMBER and AM1 partial charges in InsightII. The steric grid representing the protein was computed using the default Autodock values with a 40 × 50 × 40 Å grid centered on the C α carbon of L302. The protein was transformed and rotated to achieve better overlapping of the docking grid with the binding site by making the orientation of the β 1 sheet and α 1 and α 7 helices approximately parallel to the y axis. Other ligands were built from the structure of BIRT-377 and optimized using AMBER and AM1 partial charges in InsightII. Autodock runs of 2.5 million genetic algorithm steps with 50 populations were performed. Only results consistent with the solvent accessibility for N-1 by X-ray crystal structure analysis and the best-energy orientations were selected for further analysis.

RESULTS

Equilibrium Binding and Off-Rate Analysis of FBABIRT. BIRT-377 has been previously shown to bind to the I domain of LFA-1 and to allosterically inhibit ligand binding (18). Structure–activity work with BIRT-377 had suggested that the hydantoin methyl group when bound to LFA-1 was oriented away from the binding site, suggesting that changes at this site would not interfere with BIRT-377 binding. After the addition of an alkyl chain and fluorescein group, we produced FBABIRT (Scheme 1).

Initial studies were conducted to determine whether FBABIRT would show increasing fluorescence with increasing concentrations (1–500 nM) when bound to HL60 cells. With this range of linear fluorescence detection, we then performed a series of experiments to determine the affinity constant of FBABIRT (parts a and b of Figure 1). The shapes

of the curves associated with specific binding were similar to those seen in receptor–ligand studies using radiolabeled small molecule ligands directed against other integrins (33). In addition, the nonspecific (blocked) binding curves were identical to those generated by purified fluorescein used at similar concentrations (data not shown). The K_d for FBABIRT was 110 nM. In the presence of Mn²⁺, a known activator of integrin activity, a slightly higher affinity was detected of 70 nM.

We confirmed these equilibrium binding results by studying the dissociation characteristics of FBABIRT over time (Figure 1c). The data were produced and fit with an exponential curve as described in the Experimental Procedures. A k_{off} of 0.037 and 0.110 sec^{−1} were observed in the presence and absence of Mn²⁺, respectively. The dissociation in the presence of Mn²⁺ was approximately 3-fold slower than in the absence of Mn²⁺, in general agreement with the equilibrium binding studies. As it has been shown previously for the VLA-4 integrin with a different ligand (LDV–FITC), the heterogeneity of the population of the receptors can be addressed using kinetic analysis of the dissociation of the fluorescent probe (FBABIRT in our case) (31). Receptors of different affinity exhibit large differences in the dissociation rates. This difference can be used to calculate fractions of receptors in each affinity state on live cells by fitting the dissociation curve to the multiexponential equations. For the case when all receptors exhibit the same affinity state, kinetics of the dissociation is single-exponential as in this case. Because the dissociation kinetics fit a single-exponential curve (Figure 3c), LFA-1 receptors, analogous to the integrin VLA-4 receptors (31), appear homogeneous with regard to the affinity state either in the presence or absence of Mn²⁺.

Specificity of FBABIRT Binding to the I Domain. To further investigate the capability of FBABIRT to specifically bind to LFA-1, we examined the binding of FBABIRT to HL60 cells in a flow cytometer (Figure 2). HL60 cells express ~300 000 LFA-1 receptors per cell (data not shown). We used BIRT-377 and mAb's R7.1 and TS1/22 to specifically study FBABIRT binding. Both mAb's R7.1 and TS1/22 have been previously shown to bind to the I domain of LFA-1. mAb R7.1 but not TS1/22 blocks BIRT-377 binding to LFA-1 (34). Specific binding of 200 nM FBABIRT was completely blocked by BIRT-377 and mAb R7.1 but not TS1/22 (Figure 2). Similar results were achieved at 100 nM FBABIRT as well (data not shown).

Structure–Activity Studies of BIRT-377 Using FBABIRT. The structure of BIRT-377 and the initial lead compound suggested that the chirality of the C on the hydantoin ring

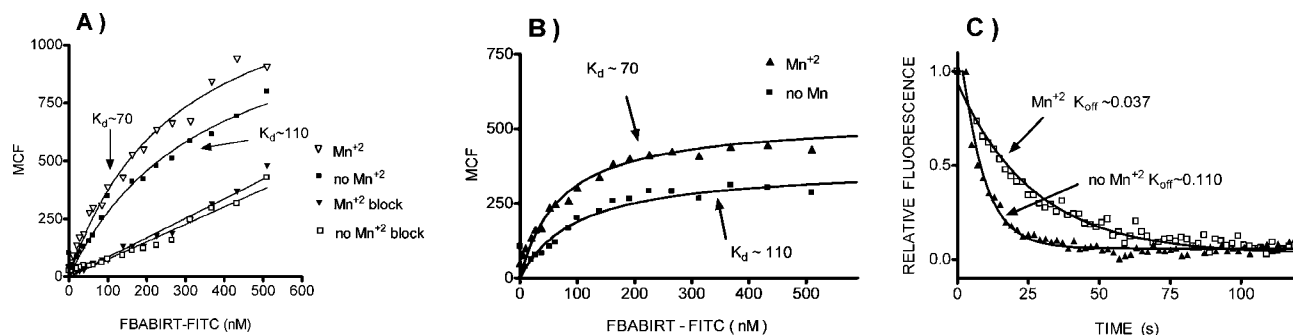


FIGURE 1: Equilibrium binding and kinetic off rate of FBABIRT in the presence of manganese. (A) Equilibrium binding experiments using HL60 cells treated with a range of concentrations (1–500 nM) of FBABIRT in the presence or absence of 1 mM MnCl_2 . Incubations were performed for short times on ice. Because the equilibration time of high-affinity molecules is typically a function of their dissociation rate, we have found it experimentally convenient to perform either 1 h or overnight incubations. Nonspecific binding was determined using a 500-fold excess of unlabeled butylamino-nor-BIRT (compound **I** in Table 1). Analysis was performed on a FACScan (Becton–Dickinson). A total of 10 000 events were acquired, and mean cell fluorescence (MCF) was graphed. All samples were run in parallel. The data are representative of three experiments. (B) Specific binding curves generated by subtracting the MCF of the blocked samples from the total fluorescent at each respective concentration of FBABIRT. (C) Off-rate experiments using HL60 cells ($1 \times 10^6 \text{ mL}^{-1}$) incubated with 100 nM FBABIRT for 30 min on ice and 500 rpm stirring. Flow cytometric analysis was performed continuously for up to 1000 s. The samples were analyzed for 30–240 s to establish a baseline, and then the stimulus (Mn^{2+}) was added and FACS acquisition was immediately re-established, losing 5–10 s of the total time course. For kinetic dissociation measurements, cell samples were preincubated with 100 nM of FBABIRT and were treated with 500-fold excess (50 μM) unlabeled butyl-amino nor-BIRT (compound **I** in Table 1), and the dissociation of FBABIRT was followed. The resulting data were converted to mean channel fluorescence over time using Tru-Rate software developed by Seamer and Sklar or using FACSQuery software developed by B. Edwards. Curve fits and statistics were performed using GraphPad Prism 6.0 (San Diego, CA) (30).

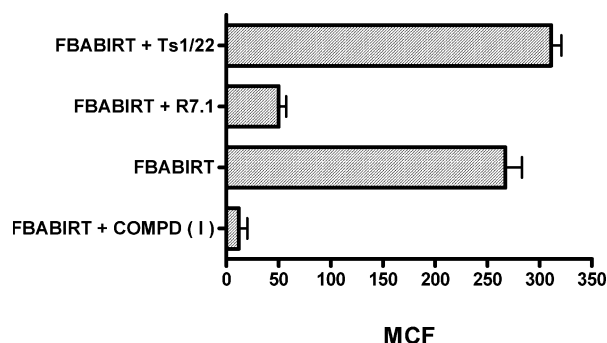


FIGURE 2: Specific binding of FBABIRT to the LFA-1 I domain. HL60 cells were incubated with FBABIRT (200 nM) in the presence or absence of mAb's or unlabeled 50 μM butylamino nor-BIRT (compound **I** in Table 1) as described in the Experimental Procedures. The mean-channel fluorescence was determined by flow cytometric analysis. As a background control, the fluorescence of cells treated with 200 nM fluorescein only was measured and subtracted from the mean channel fluorescence of each sample. The experiment was repeated 3 times. The average values with standard deviations are shown.

and methylation at the N-1 amide nitrogen could be important in the structure function activity of BIRT-377. Accordingly, we next examined structure–affinity relationships of BIRT-377 by examining the binding of FBABIRT over a 4 log concentration range of several BIRT-377 derivatives (Table 1). An EC_{50} (concentration of half-maximal inhibition) was determined using 100 nM FBABIRT. The chirality of the C-5 carbon affected the activity, with the *S* enantiomer having an affinity 2–4-fold more potent than those of the *R* enantiomers (**III** versus **IV** and **V** versus **VI**). Also, the presence of an N-1 methyl (**VI** and **V**) and N-1 pentyl amino substituent (**II**) modestly increased potency for each enantiomer (**VI** versus **IV** and **V** versus **III**). Interestingly, the addition of a second methyl group at the C-5 carbon and para-bromo benzyl group dramatically improved potency (**I** versus **V**). Because immunologic and crystallographic studies have shown that the C-5 methyl group of BIRT-377 is oriented toward the solvent and does not interact with the I

domain (18), the ~23-fold increase in potency (**I** versus **V**) is likely the result of the additional para-bromo benzyl moiety as well as an alteration in conformation of the small molecule because of the additional C-5 methyl group (see the modeling studies below).

These binding results were compared with the ability of the compounds to inhibit homotypic aggregation of JY cells (Table 1). These cells have been previously shown to aggregate in a LFA-1-dependent manner. An IC_{50} (half-maximal inhibition of cell aggregation) was determined by measuring the degree of aggregation over a 3 log concentration range, analogous to the FBABIRT-binding studies performed in Figure 3. There was qualitative agreement between the affinity measurements of each derivative and its ability to block cellular aggregation with the exception of compound **I**, which did not inhibit homotypic aggregation. However, the relationship of cellular and molecular inhibition was not linear, presumably reflecting the multivalency of the cell aggregation assay versus the monovalency of the competition assays.

Modeling of BIRT Derivatives into the I Domain. To examine the structure–activity relationships of BIRT-377 and its derivatives, we docked each compound to the I domain in a manner analogous to previous work based on immunologic and X-ray crystallographic findings (Figure 4) (18). BIRT-377 and its derivatives dock to the same site as previously described (18). BIRT-377, nor-BIRT (**I**), and Butyl-amino-nor-BIRT (**II**) had very similar docked structures (rmsd < 0.1 Å). Other derivatives had a higher energy of docking compared to these three, but the range of their predicted binding energy was too narrow to correlate with affinity measurements (data not shown). Compounds **III** and **IV** represent isomeric structures (*S* and *R* forms, respectively) of the lead compound from which BIRT-377 was derived (Figure 4a). In the docking results, both compounds (**III** and **IV**) have a more extended conformation that inserts the free phenyl group inserted deeper into a hydrophobic pocket that

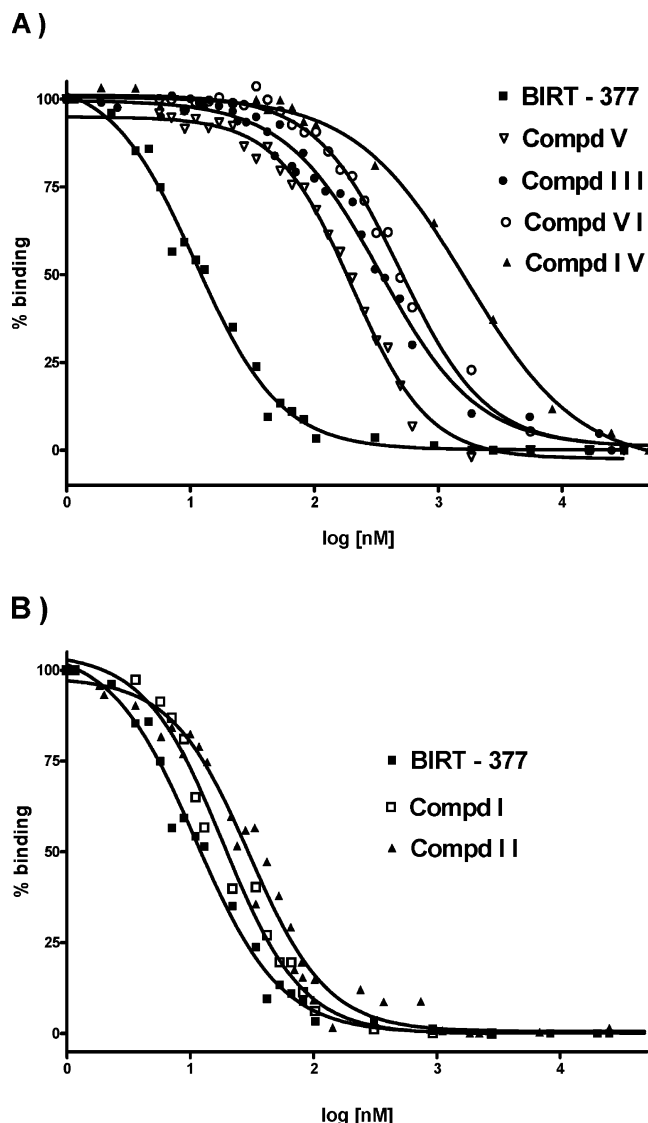


FIGURE 3: Representative curves of competition analysis between FBABIRT and BIRT derivatives. Aliquots of HL-60 cells were incubated for 1 h on ice with 100 nM FBABIRT and increasing concentrations of BIRT derivatives as indicated and described in the Experimental Procedures. Lower affinity (A) and higher affinity (B) derivatives are grouped. BIRT-377 is shown in both set of curves for comparison purposes. The MCF was measured by flow cytometry. The percent binding was calculated according to the following formula: percent binding = (MCF derivative – MCF total block)/(MCF 0 block – MCF total block). The log of the concentration of the BIRT derivative was plotted against the percent binding, and the EC_{50} was calculated using the Prism software. Each EC_{50} value (Table 1) presents the mean \pm standard deviation of at least three independent experiments.

interacts with Y257, I259, L298, and I235. Compound IV, which shows the lowest affinity, is inserted deepest into this hydrophobic pocket, presumably causing steric clashes and hence lower affinity. The addition of the N-1 methyl group on the central hydantoin ring leads to isomeric derivatives (V and VI) that have a docked conformation similar to BIRT-377 (Figure 4b). The conformation of compound V (*S* form) overlays well with BIRT-377, but the unsubstituted phenyl ring appears to interact with the solvent not with Y166. We hypothesize that this explains the lower affinity interaction of this compound. In contrast, compound VI is rotated 180° in comparison to BIRT-377 and compound V so that the dichlorophenyl group overlaps with the para-bromo group

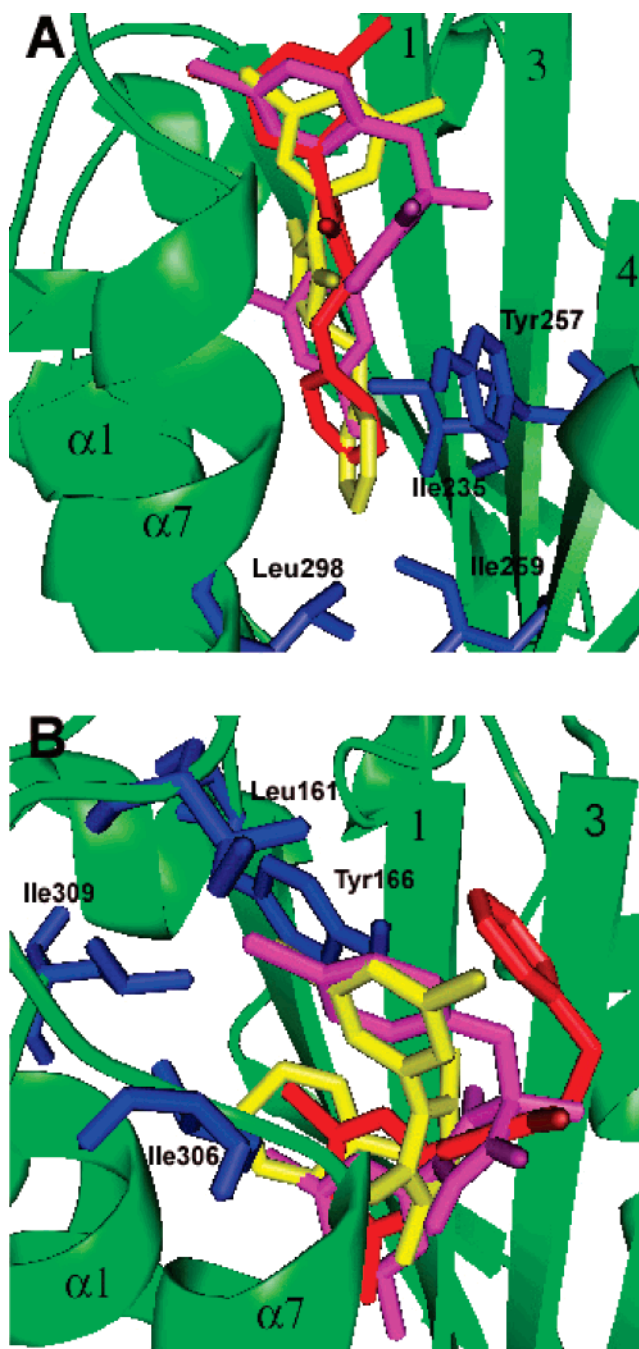


FIGURE 4: BIRT and derivatives docked to the I domain of LFA-1. (A) Compounds III (red) and IV (yellow) docked to the I domain. These structures represent the enantiomeric structures of the lead compound from which BIRT-377 was derived. The hydrophobic pocket composed of Y257, I235, L298, and I259 into which they extend is shown. BIRT-377 is shown in violet for the purpose of comparison to emphasize its relative bent conformation and the extension of compounds III and IV into the hydrophobic pocket. (B) Compounds V (red) and VI (yellow) docked to the I domain. For comparison purposes, BIRT-377 is shown in violet. Compound VI is rotated 180° but retains a similar bound conformation and amino acid interfaces. Compound V does not show the interaction with Y166 that is present for BIRT-377, which likely leads to higher affinity. Docking was performed as described in the Experimental Procedures.

of BIRT-377. Although this is a dramatic rotation, the conformation of compound VI and its interactions with the putative binding site amino acid residues remain similar to those of BIRT-377 (Figure 4b).

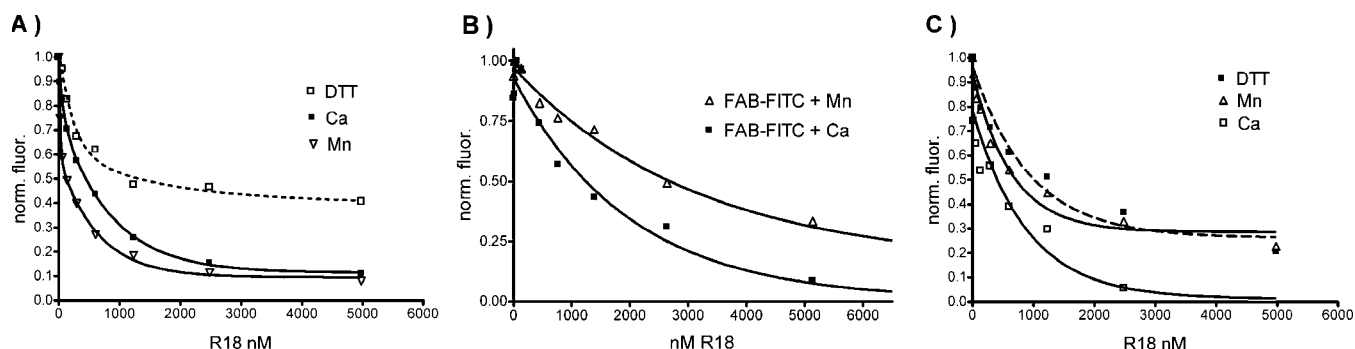


FIGURE 5: FRET experiments. (A) Energy-transfer measurements using FBABIRT. HL-60 cells were incubated with 200 nM FBABIRT for 30 min at 37 °C, in the presence or absence of DTT or Mn^{2+} as described in the Experimental Procedures. Fluorescent intensity is measured as a function of the R18 concentration. (B) Energy-transfer experiments using FITC-labeled TS1/22 Fab fragments (anti-LFA-1 α subunit I domain). HL60 cells were incubated with 50 nM FITC-labeled TS1/22 Fab overnight at 4 °C in the presence or absence of Mn^{2+} as described in the Experimental Procedures. Samples were warmed to 37 °C for 30 min prior to evaluation. (C) Energy-transfer measurements using the FITC-LDV peptide. The same process as in A is repeated for detecting VLA-4 height changes using U937 Δ ST cells and 4 nM LDV-FITC. Representative data of four experiments is shown.

FRET Experiments. Dynamic changes in the height (i.e., conversion from bent to extended forms) of the LFA-1 molecule were examined using FRET. Using a FITC-labeled peptide bound to VLA-4 and rhodamine lipid incorporated into the cell membranes, we have previously shown that we can detect changes in the vertical distance between the integrin head and surface of the plasma membrane as they convert from the bent to extended forms in the presence of dithiothreitol (DTT) or divalent cation (28, 29). DTT has been thought to promote the extension of the integrin by reducing cysteine disulfide bonds (32). With an analogous approach, we examined the height changes in LFA-1 on HL60 cells, and in parallel, the height change of VLA-4 was measured with identical stimuli (Figure 5). A decrease in quenching efficiency, corresponding to the extension of the molecule, was detected on VLA-4 when $MnCl_2$ or DTT was used as previously described (Figure 5c) (31, 32). An extension of BIRT-bound LFA-1 was detected in the presence of DTT (Figure 5a). However, an increase in fluorescence was not detected in the presence of $MnCl_2$, indicating that BIRT-bound LFA-1 does not extend in the presence of $MnCl_2$. To demonstrate that LFA-1 in the absence of BIRT-377 could extend with activation, we examined the ability of LFA-1 to extend in the presence of $MnCl_2$ using FITC-labeled TS1/22 Fab fragments (Figure 5b). These Fab fragments bind to the I domain of the α subunit of LFA-1. In the presence of $MnCl_2$, LFA-1 was extended away from the rhodamine-labeled cell surface in comparison to LFA-1 in the absence of $MnCl_2$.

Examination of FBABIRT Binding in the Presence of Mn^{2+} and DTT. Because our data suggested that BIRT-bound LFA-1 would convert from a bent form to an extended form in the presence of DTT but not $MnCl_2$, we wished to determine whether the binding of FBABIRT to LFA-1 in the presence of DTT and $MnCl_2$ also changed (Figure 6). FBABIRT binding to unstimulated cells was specifically blocked by unlabeled BIRT and the mAb R7.1. TS1/22, a mAb directed against the I domain of the α subunit that does not compete with BIRT binding, did not block FBABIRT binding. Exposure of cells to $MnCl_2$ but not DTT leads to increased FBABIRT binding in comparison to untreated cells. Binding of FBABIRT in the presence of DTT and $MnCl_2$ was comparable to $MnCl_2$ alone. In all cases, the binding

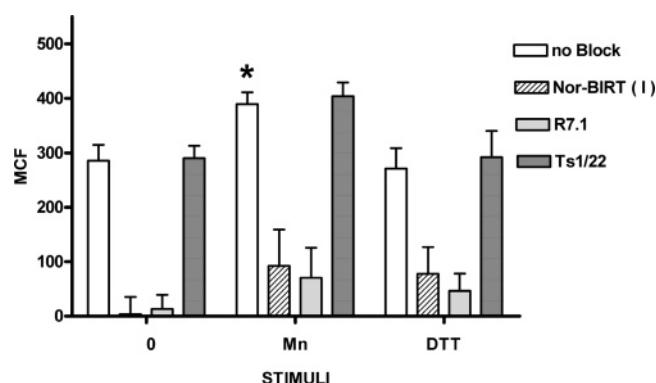


FIGURE 6: Binding of FBABIRT to HL60 cells in the presence of $MnCl_2$ and DTT. HL60 cells are incubated with 200 nM FBABIRT for 60 min at 37 °C in the presence or absence of $MnCl_2$ or DTT as described in the Experimental Procedures. Unlabeled nor-BIRT (I) or mAb directed against the LFA-1 I domain (R7.1 and TS1/22) were added as indicated. For experiments performed in the presence of DTT, all samples (DTT treated as well as samples subjected to other conditions) were incubated at 37 °C for 60 min. As a background control, the fluorescence of cells treated with 200 nM fluorescein only was measured and subtracted from the mean channel fluorescence of each sample. The experiment was repeated 6 times, and the standard deviation is shown. An asterisk indicates $p < 0.05$ between the fluorescence of FBABIRT bound LFA-1 in the presence of Mn^{2+} compared with FBABIRT bound in the absence of Mn^{2+} .

was specifically blocked by unlabeled nor-BIRT (I) or the mAb R7.1.

DISCUSSION

Integrins exist in distinct conformations that generate varying affinity for the ligand. Integrins have a switchblade-like opening that corresponds to a conversion from a bent form of lower affinity to an extended form of higher affinity for the native ligand (Figure 7). The α subunit of integrins has 2 structural forms; those that contain I domains and those that do not. Recently, we and others have used small molecules to probe these conformational changes in a non-I-domain-containing integrin, VLA-4 (28, 29). In this study, we use a small molecule allosteric inhibitor to examine conformational changes in the I-domain-containing integrin LFA-1. We also perform a series of structure-activity relationship and computational docking studies that indicate BIRT-377 is likely a fully optimized inhibitor. We show that

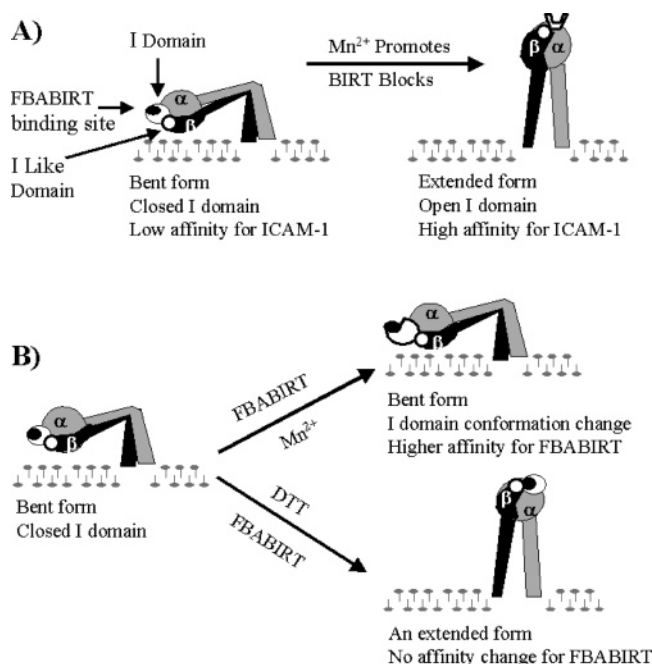


FIGURE 7: Schematic of LFA-1 conformational changes in the presence of FBABIRT, DTT, and $MnCl_2$. (A) LFA-1 extends in the presence of $MnCl_2$ and LFA-1 extension blocked by FBABIRT consistent with the findings of other investigators. (B) FBABIRT prevents the extension of LFA-1 induced by $MnCl_2$, but $MnCl_2$ increases the affinity of LFA-1 for FBABIRT. DTT promotes the extension of LFA-1 in the presence of FBABIRT, but an increase in binding of FBABIRT is not detected.

$MnCl_2$ induces the switchblade opening of LFA-1 (Figure 7). When the bent form of LFA-1 is stabilized by FBABIRT, we can detect a modest change in affinity of LFA-1 for FBABIRT in the presence of $MnCl_2$. This observation suggests that the I domain may undergo a modest conformational change in the bent form in the presence of $MnCl_2$. Furthermore, the stabilization of LFA-1 by BIRT-377 can be overcome with DTT treatment, indicating that there is the possibility of pharmaceutically separating the I domain conformational changes from the global switchblade changes.

The equilibrium binding curves generated using this fluorescent technology are comparable to curves generated using radiolabeled ligands with other integrins (33). Our observations indicate that FBABIRT has a $K_d \sim 110$ nM with $k_{off} \sim 0.110$ sec $^{-1}$. The calculated $k_{on} \sim 1 \times 10^{-6}$ M $^{-1}$ s $^{-1}$ is also in agreement with that observed for other small molecule–receptor interactions (35). Because the concentration of FBABIRT used in competition assays (100 nM) was similar to its affinity constant, the EC_{50} determined for BIRT-377 in Table 1 should also be an estimation of its affinity constant. Our observed value of 13.7 ± 4 nM is in agreement with previous studies that estimated a K_d of 25.8 ± 6.4 nM (36). It is quite remarkable that flow cytometry permits the homogeneous analysis of ligand binding at concentrations up to 500 nM FBABIRT. This situation is made possible by the fact that the binding signal is associated with a fluorescent pulse above a direct current signal as each particle transit of the laser beam. The validity of the analysis requires that the nonspecific (background) signal is linear over the entire concentration. Linearity is maintained by reducing the voltage (500–600 V) on the photomultiplier tubes so that they do not saturate during data acquisition.

Previous work has indicated that at least three states exist for LFA-1, a bent conformer with closed I domain (receptor with low affinity for native ligand), an extended conformer with a closed headpiece (intermediate affinity), and an extended conformer with an open I domain (high affinity) (12, 16, 37). Mn^{2+} activates all integrins, apparently by binding to the MIDAS domain of the I-like domain of the β subunit (37). It has been postulated that the binding of Mn^{2+} to the β subunit leads to a shift of the molecule from a bent conformer with a closed α subunit I domain to an extended conformer with an open I domain (31). Our FRET results demonstrate that this switchblade opening of LFA-1 does occur in the presence of Mn^{2+} . Although Mn^{2+} binds to the extracellular segment of integrins, it appears in many respects to mimic inside-out signaling, both by activating in the absence of bound ligand and by exposing a similar array of activation epitopes (38, 39). In this study, we also provide indirect evidence that Mn^{2+} binding to the β subunit leads to a conformational shift in the I domain of the α subunit. A small affinity and off-rate change in FBABIRT binding can be detected in the presence of Mn^{2+} , suggesting that the conformational change in the I domain is modest. Because FBABIRT stabilizes the bent form as indicated by our FRET results and suggested by the work of others (18, 19, 21, 22), the conformational change in the I domain likely occurs without the molecule extending.

BIRT-377 stabilization of the bent conformer can be overcome by DTT treatment, which extends the molecule. Although the magnitude of the FRET signal will correspond to the height change, there is considerable uncertainty in the precise distances using this technology. Our previous studies on VLA-4 have estimated that there are <50 Å between the headpiece of the integrin and the cell membrane with Mn^{2+} stimulation, while Mn^{2+} plus DTT leads to further extension with <100 Å separating the headpiece from the cell membrane (32). On the basis of these estimates, LFA-1 I domain would be ~ 25 – 50 Å from the cell membrane after DTT stimulation.

X-ray crystallography and computer-modeling studies indicate that the I domain is accessible to native ligand in the bent or extended forms (16, 17, 40), although there are an order of magnitude off-rate and affinity differences in ICAM-1 binding to either bent (low affinity for native ligand) or extended (high affinity for native ligand) forms (38, 41). Thus, it appears that ICAM-1 may bind weakly to the α L I domain in the closed or intermediate conformation as well as the open conformation. Binding of ICAM-1 then presumably favors a shift to the open conformation (16, 17, 40). BIRT-377 stabilizes the bent form as shown by suppression of epitope induction by Mn^{2+} and does not directly compete with ICAM-1 binding. The conversion from bent to extended forms is presumably disrupted by BIRT-377, preventing the α 7 helix movement of the I domain after ligand binding or activation. Thus, it should be possible to bind native ICAM-1 to low-affinity LFA-1 in the presence of BIRT-377, but physiologic activity that requires an extended or higher affinity state of LFA-1 would be prevented. It would be of interest to perform these types of studies in the future using BIRT-377 and LFA-1 or ICAM-1 engineered to have a fluorescent probe in known amino acid positions.

Our structure–activity and docking studies provide an explanation for the relative affinities of BIRT-377, the lead

compound from which it was derived, and several derivatives. In addition, our docking studies suggest that it is unlikely that further optimization of the BIRT-377 scaffold will yield an increase in binding affinity. The initial lead compounds (**III** and **IV**) were more extended in their conformation and disrupted a hydrophobic pocket (defined by Y257, I259, I235, and F245) between the first and seventh α helices of the I domain. These docking studies suggest that deeper penetration into this pocket resulted in the loss of potency. Adding N-1 methyl or N-1 pentyl amino substituent results in a bent conformation of the small molecules that avoids the hydrophobic pocket into which the lead compounds extend, resulting in increased potency. With the addition of a methyl group to the hydantoin ring and *S* form of the unsubstituted phenyl group, the small molecule assumes a more bent conformation that interacts with interface amino acid residues away from the hydrophobic pocket. The *R* form is docked with a 180° rotation in comparison to the bound *S* form, while maintaining a similar bound conformation and similar side-chain interactions. The addition of a second methyl group and a para-bromo group on BIRT-377 in comparison to compound **V** leads to further favorable bending and interaction of the unsubstituted phenyl with Y166 instead of interacting with the solvent. In the docked, bound conformation, additional favorable interactions of BIRT-377 with the I domain are not apparent, suggesting a fully optimized structure. It is curious that nor-BIRT (**I**) is a potent inhibitor of BIRT-377 binding but does not block cell aggregation. The absence of the methyl group makes the compound labile to pH, and it may have a considerably shorter half-life at pH 7.4, the pH at which the cellular aggregation assays are performed.

LFA-1 and other $\beta 2$ integrins are much more adept at supporting firm adhesion of leukocytes to endothelium. However, recent observations have indicated that LFA-1 also contributes to rolling of leukocytes as well (17). It appears that the extended form of $\alpha \beta 2$ favors cellular adhesion and that the conformation of the $\beta 2$ I-like domain regulates the conformation of the α subunit I domain and whether it supports rolling or firm adhesion. Thus, rolling can occur on extended $\alpha \beta 2$ in the absence of activation that leads to the high-affinity form of the I domain. With the recent introduction of new small molecules that bind the $\beta 2$ I-like domain that may induce rolling or prevent firm adhesion, it will be of interest to study conformational changes of the $\alpha \beta 2$ molecule using the fluorochrome-labeled derivatives to further refine our understanding of the conformational changes in integrins and their physiologic consequences.

ACKNOWLEDGMENT

The shared UNM flow facility in which these experiments were performed is partially supported by the Cigarette Tax, UNM CRTC, and NIH CA88339. UNM Division of Bio-computing is supported by New Mexico Tobacco Settlement funds.

REFERENCES

- Giancotti, F. G., and Ruoslahti, E. (1999) Integrin signaling, *Science* 285, 1028–1032.
- Schwartz, M. A., and Ginsberg, M. H. (2002) Networks and crosstalk: Integrin signalling spreads, *Nat. Cell Biol.* 4, E65–E68.
- Larson, R. S., and Springer, T. A. (1990) Structure and function of leukocyte integrins, *Immunol. Rev.* 114, 181–217.
- Gahmberg, C. G., Tolvanen, M., and Kotovuori, P. (1997) Leukocyte adhesion—structure and function of human leukocyte $\beta 2$ -integrins and their cellular ligands, *Eur. J Biochem.* 245, 215–232.
- Shimaoka, M., Lu, C., Palframan, R. T., von Andrian, U. H., McCormack, A., Takagi, J., and Springer, T. A. (2001) Reversibly locking a protein fold in an active conformation with a disulfide bond: Integrin αL I domains with high affinity and antagonist activity *in vivo*, *Proc. Natl. Acad. Sci. U.S.A.* 98, 6009–6014.
- Anderson, D. C., and Springer, T. A. (1987) Leukocyte adhesion deficiency: An inherited defect in the Mac-1, LFA-1, and p150, 95 glycoproteins, *Annu. Rev. Med.* 38, 175–194.
- Nicolls, M. R., Coulombe, M., Beilke, J., Gelhaus, H. C., and Gill, R. G. (2002) CD4-dependent generation of dominant transplantation tolerance induced by simultaneous perturbation of CD154 and LFA-1 pathways, *J Immunol.* 169, 4831–4839.
- Poston, R. S., Robbins, R. C., Chan, B., Simms, P., Presta, L., Jaldieu, P., and Morris, N. E. (2000) Effects of humanized monoclonal antibody to rhesus CD11a in rhesus monkey cardiac allograft recipients, *Transplantation* 69, 2005–2013.
- Sarnacki, S., Auber, F., Cretolle, C., Camby, C., Cavazzana-Calvo, M., Muller, W., Wagner, N., Brousse, N., Revillon, Y., Fischer, A., and Cerf-Bensussan, N. (2000) Blockade of the integrin $\alpha L \beta 2$ but not of integrins $\alpha 4$ and/or $\beta 7$ significantly prolongs intestinal allograft survival in mice, *Gut* 47, 97–104.
- Gottlieb, A. B., and Bos, J. D. (2002) Recombinantly engineered human proteins: Transforming the treatment of psoriasis, *Clin. Immunol.* 105, 105–116.
- Gottlieb, A. B., Krueger, J. G., Wittkowski, K., Dedrick, R., Walicke, P. A., and Garovoy, M. (2002) Psoriasis as a model for T-cell-mediated disease: immunobiologic and clinical effects of treatment with multiple doses of efalizumab, an anti-CD11a antibody *Arch. Dermatol.* 138, 591–600.
- Shimaoka, M., Takagi, J., and Springer, T. A. (2002) Conformational regulation of integrin structure and function, *Annu. Rev. Biophys. Biomol. Struct.* 31, 485–516.
- Xiong, J. P., Stehle, T., Diefenbach, B., Zhang, R., Dunker, R., Scott, D. L., Joachimiak, A., Goodman, S. L., and Arnaout, M. A. (2001) Crystal structure of the extracellular segment of integrin $\alpha V \beta 3$, *Science* 294, 339–345.
- Huang, C., Zang, Q., Takagi, J., and Springer, T. A. (2000) Structural and functional studies with antibodies to the integrin $\beta 2$ subunit. A model for the I-like domain, *J. Biol. Chem.* 275, 21514–21524.
- Lee, J. O., Rieu, P., Arnaout, M. A., and Liddington, R. (1995) Crystal structure of the A domain from the α subunit of integrin CR3 (CD11b/CD18), *Cell* 80, 631–638.
- Shimaoka, M., Xiao, T., Liu, J. H., Yang, Y., Dong, Y., Jun, C. D., McCormack, A., Zhang, R., Joachimiak, A., Takagi, J., Wang, J. H., and Springer, T. A. (2003) Structures of the αL I domain and its complex with ICAM-1 reveal a shape-shifting pathway for integrin regulation, *Cell* 112, 99–111.
- Salas, A., Shimaoka, M., Kogan, A. N., Harwood, C., von Andrian, U. H., and Springer, T. A. (2004) Rolling adhesion through an extended conformation of integrin $\alpha L \beta 2$ and relation to αI and βI -like domain interaction, *Immunity* 20, 393–406.
- Last-Barney, K., Davidson, W., Cardozo, M., Frye, L. L., Grygon, C. A., Hopkins, J. L., Jeanfavre, D. D., Pav, S., Qian, C., Stevenson, J. M., Tong, L., Zindell, R., and Kelly, T. A. (2001) Binding site elucidation of hydantoin-based antagonists of LFA-1 using multidisciplinary technologies: Evidence for the allosteric inhibition of a protein–protein interaction, *J. Am. Chem. Soc.* 123, 5643–5650.
- Kallen, J., Welzenbach, K., Ramage, P., Geyl, D., Kriwacki, R., Legge, G., Cottens, S., Weitz-Schmidt, G., and Hommel, U. (1999) Structural basis for LFA-1 inhibition upon lovastatin binding to the CD11a I-domain, *J. Mol. Biol.* 292, 1–9.
- Liu, G., Huth, J. R., Olejniczak, E. T., Mendoza, R., DeVries, P., Leitza, S., Reilly, E. B., Okasinski, G. F., Fesik, S. W., and von Geldern, T. W. (2001) Novel *p*-arylthio cinnamides as antagonists of leukocyte function-associated antigen-1/intracellular adhesion molecule-1 interaction. 2. Mechanism of inhibition and structure-based improvement of pharmaceutical properties, *J. Med. Chem.* 44, 1202–1210.
- Lu, C., Shimaoka, M., Zang, Q., Takagi, J., and Springer, T. A. (2001) Locking in alternate conformations of the integrin $\alpha L \beta 2$

- I domain with disulfide bonds reveals functional relationships among integrin domains, *Proc. Natl. Acad. Sci. U.S.A.* 98, 2393–2398.
22. Weitz-Schmidt, G., Welzenbach, K., Brinkmann, V., Kamata, T., Kallen, J., Bruns, C., Cottens, S., Takada, Y., and Hommel, U. (2001) Statins selectively inhibit leukocyte function antigen-1 by binding to a novel regulatory integrin site, *Nat. Med.* 7, 687–692.
23. Burdick, D. J. (99 A.D.) Antagonists for treatment of CD11/CD18 adhesion receptor mediated disorders, WO9949856.
24. Burdick, D. J., Gadek, T. R., Marsters, J., Oare, D. A., Reynolds, M. E., and Stanley, M. S. (2001) LFA-1 antagonists compounds, WO02059114.
25. Fotouhi, N., Gillespie, P., Guthrie, R., Pietranico-Cole, S., and Yun, W. (1999) Diaminopropionic acid derivatives, WO021920.
26. Fotouhi, N., Gillespie, P., Guthrie, R., Pietranico-Cole, S., and Yun, W. F. (2001) Dehydroamino acids, WO0158853.
27. Davidson, W., Hopkins, J. L., Jeanfavre, D. D., Barney, K. L., Kelly, T. A., and Grygon, C. A. (2003) Characterization of the allosteric inhibition of a protein–protein interaction by mass spectrometry, *J. Am. Soc. Mass Spectrom.* 14, 8–13.
28. Chigaev, A., Blenc, A. M., Braaten, J. V., Kumaraswamy, N., Kepley, C. L., Andrews, R. P., Oliver, J. M., Edwards, B. S., Prossnitz, E. R., Larson, R. S., and Sklar, L. A. (2001) Real time analysis of the affinity regulation of $\alpha 4$ -integrin. The physiologically activated receptor is intermediate in affinity between resting and Mn^{2+} or antibody activation, *J. Biol. Chem.* 276, 48670–48678.
29. Chigaev, A., Zwart, G., Graves, S. W., Dwyer, D. C., Tsuji, H., Foutz, T. D., Edwards, B. S., Prossnitz, E. R., Larson, R. S., and Sklar, L. A. (2003) $\alpha 4\beta 1$ integrin affinity changes govern cell adhesion, *J. Biol. Chem.* 278, 38174–38182.
30. Curley, G. P., Blum, H., and Humphries, M. J. (1999) Integrin antagonists, *Cell Mol. Life Sci.* 56, 427–441.
31. Chigaev, A., Buranda, T., Dwyer, D. C., Prossnitz, E. R., and Sklar, L. A. (2003) FRET detection of cellular $\alpha 4$ -integrin conformational activation, *Biophys. J.* 85, 3951–3962.
32. Chigaev, A., Zwart, G. J., Buranda, T., Edwards, B. S., Prossnitz, E. R., and Sklar, L. A. (2004) Conformational regulation of $\alpha 4\beta 1$ -integrin affinity by reducing agents. “Inside-out” signaling is independent of and additive to reduction-regulated integrin activation, *J. Biol. Chem.* 279, 32435–32443.
33. Chen, L. L., Whitty, A., Lobb, R. R., Adams, S. P., and Pepinsky, R. B. (1999) Multiple activation states of integrin $\alpha 4\beta 1$ detected through their different affinities for a small molecule ligand, *J. Biol. Chem.* 274, 13167–13175.
34. Woska, J. R., Jr., Shih, D., Taqueti, V. R., Hogg, N., Kelly, T. A., and Kishimoto, T. K. (2001) A small-molecule antagonist of LFA-1 blocks a conformational change important for LFA-1 function, *J. Leukocyte Biol.* 70, 329–334.
35. Benveniste, M., and Mayer, M. L. (1991) Structure–activity analysis of binding kinetics for NMDA receptor competitive antagonists: The influence of conformational restriction, *Br. J. Pharmacol.* 104, 207–221.
36. Kepley, C. L., Cambier, J. C., Morel, P. A., Lujan, D., Ortega, E., Wilson, B. S., and Oliver, J. M. (2000) Negative regulation of Fc ϵ RI signaling by Fc γ RII costimulation in human blood basophils, *J. Allergy Clin. Immunol.* 106, 337–348.
37. Xiong, Y. M., Haas, T. A., and Zhang, L. (2002) Identification of functional segments within the $\beta 2$ I-domain of integrin $\alpha M\beta 2$, *J. Biol. Chem.* 277, 46639–46644.
38. Labadia, M. E., Jeanfavre, D. D., Caviness, G. O., and Morelock, M. M. (1998) Molecular regulation of the interaction between leukocyte function-associated antigen-1 and soluble ICAM-1 by divalent metal cations, *J. Immunol.* 161, 836–842.
39. Takagi, J., Petre, B. M., Walz, T., and Springer, T. A. (2002) Global conformational rearrangements in integrin extracellular domains in outside-in and inside-out signaling, *Cell* 110, 599–611.
40. Shimaoka, M., Salas, A., Yang, W., Weitz-Schmidt, G., and Springer, T. A. (2003) Small molecule integrin antagonists that bind to the $\beta 2$ subunit I-like domain and activate signals in one direction and block them in the other, *Immunity* 19, 391–402.
41. Tominaga, Y., Kita, Y., Satoh, A., Asai, S., Kato, K., Ishikawa, K., Horiuchi, T., and Takashi, T. (1998) Affinity and kinetic analysis of the molecular interaction of ICAM-1 and leukocyte function-associated antigen-1, *J. Immunol.* 161, 4016–4022.
42. Kelly, T. A., Jeanfavre, D. D., McNeil, D. W., Woska, J. R., Jr., Reilly, P. L., Mainolfi, E. A., Kishimoto, K. M., Nabozny, G. H., Zinter, R., Bormann, B. J., and Rothlein, R. (1999) Cutting edge: A small molecule antagonist of LFA-1-mediated cell adhesion, *J. Immunol.* 163, 5173–5177.
43. Oi, V. T., and Herzenberg, T. (1980) Immunoglobulin-producing hybrid cell lines, in *Selected Methods in Cellular Immunology* (Mishell, B. B., and Shiigi, S. M., Eds.) p 351, New York, WH Freeman, New York.

BI048187K